UDC 533.6.01

K. ALHUSSAN[1], T. V. SIDOROVICH[2], A. D. CHORNY[2]

SUPERSONIC INVISCID FLOW AROUND BODIES OF REVOLUTION: EMPIRICAL VS. NUMERICAL COMPUTATION

[1]King Abdulaziz City for Science and Technology, Kingdom of Saudi Arabia
[2]A. V. Luikov Heat and Mass Transfer Institute of NAS of Belarus

(Received 10.10.2014)

Introduction. Aerodynamic characteristics of flying vehicles shaped as bodies of revolution with a curvilinear surface generator are interested first of all to find parameters of flow around a body. On the one hand, it is necessary to analyze, from a practical point of view, aerodynamic characteristics of such vehicles moving along different trajectories in the earth's atmosphere. On the other hand, if supersonic flows are considered, it is needed to study complex flow phenomena around a body, specifically related to oblique shock wave and contact (slip) surface. Shock waves and contact surfaces are discontinuities in fluid dynamics problems [1]. The features of supersonic flow start manifesting themselves markedly for different-shape bodies (sphere, cone, cylinder, disc, etc.) at sufficiently large, but different Mach numbers M. The boundary separating a supersonic flow from a hypersonic one is highly conditional. Some of the characteristic properties of hypersonic flows appear in the vicinity of the nose of a blunt body already at $M = 3$ [1, 2].

The presence of shock waves is the main feature of flow when a thin pointed or a blunt body moves at supersonic speeds upstream [1, 2]. Flow is considered to be undisturbed up to some boundary in the vicinity of the body nose. The front part of the body is enveloped by the shock wave propagating downstream in the form of a slightly expanding surface. Flow parameters along the compression shock remain invariable. Of main interest are the features of a narrow region between the shock wave and the body. It is called the shock layer. In this layer, temperature and pressure will be much larger than those in the undisturbed flow; temperature and pressure ratios can infinitely grow with increasing Mach number. On the contrary, the density ratio is limited, although the shock layer density is larger than the undisturbed flow density. Therefore, the physical meaning of the formation of a compression shock (shock wave) consists in separating undisturbed and disturbed gas flow regions. Far behind the body, the shock wave becomes weak, whereas downstream the rear wake is positioned. As the compression shock moves farther and farther away from the body, it transits into a wave of weak disturbances [1, 2]. In addition to the shock wave, another type of discontinuity termed as a contact surface is an interface that separates two flow regions, but moves with those regions. The velocity and the pressure of the gas on each side of the contact surface are the same, but the other thermodynamic properties may be different. Unlike the shock wave, there is no flow of the gas across the contact surface [1, 2].

It is essential to evaluate the abilities of the computational fluid dynamics (CFD) technique that can solve problems in which shocks and contact surfaces occur. In particular, it is necessary to understand the details of the construction of a numerical mesh, which will allow discontinuities to be resolved [3]. When new CFD software is under development, there always arises the question of confidence of numerical computation results obtained by use of this software. The validity of the results obtained can be determined in three ways: a) comparison with the tabular data for a considered body; b) comparison with the analytical formulas obtained within the framework of the theory of supersonic inviscid gas flows; c) comparison with the numerical computation results obtained with the use of well-known reliable software.

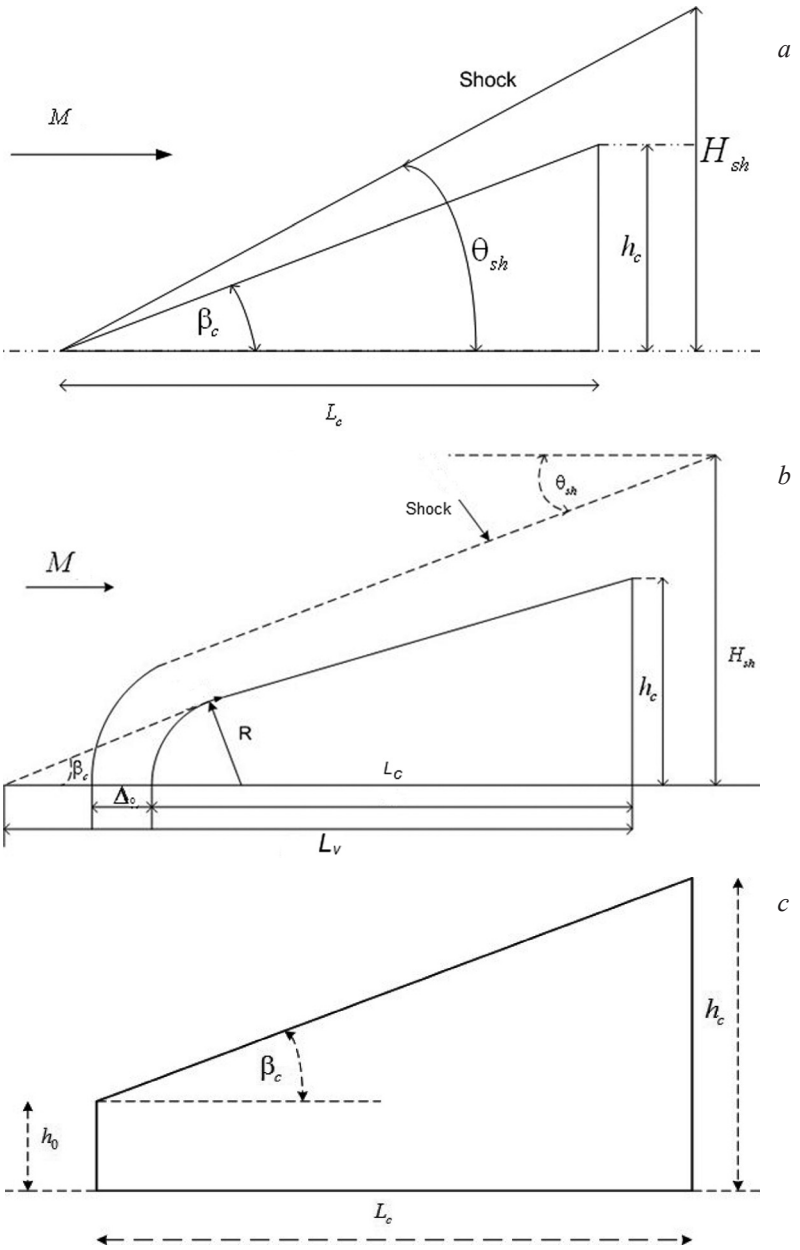

Fig. 1. Parameters of flow around circular cone (*a*), circular cone with the spherically blunt nose of radius *R* (*b*), and truncated cone (*c*) at zero angle of attack (α = 0)

The objective of the present work is to model aerodynamic processes involving the supersonic movement of an axis-symmetrical body having a conical shape in the air environment at zero angle of attack with the implication of CFD [4]. It is assumed to obtain reasonable data on aerodynamic characteristics of a circular cone, a circular cone with a spherical nose, and a truncated cone (Fig. 1) at zero angle of attack (α = 0) and to analyze their accuracy in comparison with the results obtained by empirical formulas in the region of their validity. It is the important confidence criterion.

It is thought that the most complete information on aerodynamic characteristics of pointed cones of different length is outlined elsewhere in works [5–9] (in the form of tables, plots, and approximate formulas for calculation of flow parameters). This is very valuable for their direct use in CFD software for supersonic flow predictions in the vicinity of bodies of revolution, as well as in Tables [10–12].

Circular cone. In supersonic flow around a circular cone, a shock shaped as a conic surface (Fig. 1, *a*) is initiated ahead of it. To define aerodynamic characteristics of a body at zero angle of attack, it is needed to calculate parameters of a gas flow between a body and a shock, as well as an inclination angle of a shock

generator. The known quantities are: β_c is the half-angle at the cone vertex (in deg); M is the Mach number of the incoming flow far from the body; L_c is the cone length; P_∞ is the pressure of the gas incoming flow far from the body; thermodynamic properties depending on the atmosphere altitude: in particular, ρ_∞ is the density of the gas incoming flow far from the body; γ is the specific heats ratio (for air $\gamma = 1.4$). It is needed to determine the following parameters: the wave drag coefficient equal to the pressure coefficient at the cone surface $c_{p,c} = (P_c - P_\infty) / (\rho_\infty V_\infty^2 / 2)$ where P_c is the pressure at the cone surface; the cone surface-to-incoming flow pressure ratio P_c / P_∞; the dimensionless density at the cone surface ρ_c / ρ_∞; the deflection angle θ_{sh} of the shock wave from the cone surface.

There are a number of analytical solutions to the above-stated problem that have been obtained in the constant density approximation [1, 5, 6]. This means that the density remains approximately constant between the body and the shock wave.

The ratio of shock layer density to density far from the cone is denoted as

$$\varepsilon = \frac{\rho_\infty}{\rho_{sh}} = \frac{\gamma - 1}{\gamma + 1}\left[1 + \frac{2}{(\gamma - 1) M^2 \sin^2 \theta_{sh}}\right].$$

In [13], the formula is proposed, which ties the quantities ε, β_c and θ_{sh} by

$$\theta_{sh} - \beta_c = 0.5 \frac{\gamma - 1}{\gamma + 1}\left[1 + \frac{2}{M^2 \theta^2_{sh} (\gamma - 1)}\right]\left(1 + \frac{\varepsilon}{12}\right)\theta_{sh}.$$

After some assumptions [14] are made, one can determine the deflection angle of the shock wave

$$\theta_{sh} = \left(\beta_c + \sqrt{\beta_c^2 + \frac{154\gamma^3 + 810\gamma^2 + 990\gamma + 350}{72(\gamma + 1)^4 M^2}}\right) \Bigg/ \left(\frac{11\gamma^2 + 50\gamma + 35}{12(\gamma + 1)^2}\right). \quad (1)$$

The shock layer thickness $\Delta = H_{sh} - h_c$ can then be calculated in terms of the following radii: $h_c = d_{con}/2 = L_c \operatorname{tg} \beta_c$ and $H_{sh} = L_c \operatorname{tg} \theta_{sh}$. The dimensionless pressure and the dimensionless density at the cone surface are as follows:

$$P_c / P_\infty = \frac{2\gamma}{\gamma + 1} M^2 \sin^2 \theta_{sh} - \frac{\gamma - 1}{\gamma + 1}, \quad \rho_c / \rho_\infty = \left(\frac{\gamma + 1}{2} M^2 \sin^2 \theta_{sh}\right) / \left(1 + \frac{\gamma - 1}{2} M^2 \sin^2 \theta_{sh}\right). \quad (2)$$

The dimensionless pressure at the cone surface is related to the wave drag coefficient: $P_c / P_\infty = 1 + c_{p,c} \gamma M^2 / 2$. To calculate the wave drag coefficient, a number of the formulas are available

$$c_{p,c} = 2 \sin^2 \beta_c / [(1 - \varepsilon / 4) \cos^2 (\theta_{sh} - \beta_c)]$$

or

$$c_{p,c} = (0.8 + M^{-2}) \beta_c^{1.7} / 500. \quad (3)$$

In the course of practical calculations over a wide range of M and β_c, these formulas yield the accuracy not worse than 5% [6]. In [5], it is defined more exactly. Better results are obtained over the ranges $1.5 < M < 5$ and $5^o < \beta_c < 25^o$ when the upper bound is set on the angles ($\beta_c < 50^o$) and the Mach numbers ($M < 7 - 8$), as well as the lower bound – on the conditions of flow around the cone. The formula, by which the estimated error of $c_{p,c}$ with respect to the one assessed by exact theory does not exceed 2–3% at $2 < M < 6$ and increases above 3–5 % at $M < 1.5$, has the following form [7]:

$$c_{p,c} = 2 \cdot \sin^2 \beta_c \, [1 + 4 / (1 + 16 \sin \beta_c \sqrt{M^2 - 1})]. \quad (4)$$

Formula (5) approximating another set of data [10] is more accurate. The formula, by which the maximum estimated error of $c_{p,c}$ does not exceed 1 % at $M > 2$ and increases not more than ~2.5 % at $M < 1.5$, has the following form:

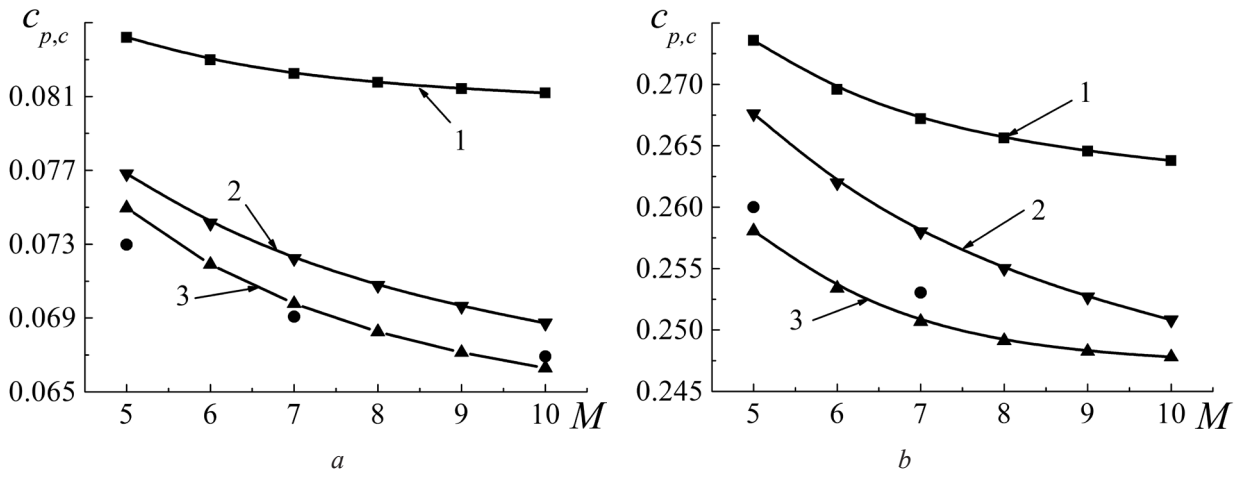

a *b*

Fig. 2. Wave drag of the circular cone vs. incoming flow Mach number (*a* – $\beta_c = 10^o$; *b* – 20^o): *1* – formula (3), *2* – (4), *3* – (5), • – numerical computation

$$c_{p,c} = 2e^x \sin^2 \beta_c \tag{5}$$

where $x = 0.18145 - y(2.0923 - y(9.092 + y(6.876 - y(62.25 + 97.1y))))$, $y = 0.1 \cdot \ln(\sin\beta_c \sqrt{M^2 - 1})$.

ANSYS Fluent 14.5 [15] was adopted to conduct a series of numerical computations for definition of gas dynamic quantities in supersonic inviscid gas flow around circular cones with half-angles β_c = 5, 10, 20^o. Comparison was made with the above-mentioned analytical formulas and a series of tables and nomograms [10–12, 14], which allowed one to define P_c / P_∞, ρ_c / ρ_∞ and θ_{sh} for pointed cones (Tab. 1). The numerical computation results for the dimensionless density and the dimensionless pressure near the cone surface coincide with the tabular values, and the analytical formulas confirm the correctness of the numerical computations performed (within 10 % of error).

Table 1. **Comparison of numerical computation results, tabular values, and analytical formulas (1), (2)**

M	β_c, ^{0}	ρ_c/ρ_∞		P_c/P_∞		θ_{sh}		
		Tables [12]	Fluent	Tables [12]	Fluent	Tables [12]	Fluent	Formula (1)
5	10	1.8022	1.796	2.3083	2.3090	15.6083	15.55	15.01
7	10	2.3092	2.276	3.3962	3.3190	13.5405	13.10	13.28
5	20	3.0370	3.027	5.5582	5.6800	24.9427	24.61	24.37
7	20	3.8707	4.010	9.6810	9.9796	23.5298	23.22	23.20

Numerical computations showed that according to the conical-flow theory, the pressure and the density at the surface of the cone retain their value, except a small region in the vicinity of its vertex. The larger the Mach number, the smaller is the angle of the shock wave departure from the cone surface. The calculation results for the wave drag obtained by analytical expressions (3)–(5) (Fig. 2) are compared with the numerical computation data. As a result, expression (5) for the wave drag coefficient of circular cones can be recommended for verification.

Cone with the spherically blunt nose. The distance Δ_0, at which the curvilinear shock wave departs from the spherical blunt nose, is determined as

$$\Delta_0 = C_0 \rho_\infty / \rho_{c0} R \tag{6}$$

where C_0 = 0.85 in [14] and 0.78 in [16], ρ_{c0} and P_{c0} are the density and the pressure near the flow stagnation point of the cone nose that are determined by the expressions:

$$\frac{\rho_\infty}{\rho_{c0}} = \frac{1 + 0.5(\gamma - 1)M_\infty^2}{P_{c0} / P_\infty},$$

$$\frac{P_{c0}}{P_\infty} = [0.5(\gamma+1)M_\infty^2]^{\frac{\gamma}{\gamma-1}} \cdot \left(\frac{\gamma+1}{2\gamma M_\infty^2 - \gamma + 1}\right)^{1/(\gamma-1)} \quad \text{or} \quad \frac{P_{c0}}{P_\infty} = 166.92 \cdot M_\infty^7 / (7M_\infty^2 - 1)^{2.5}.$$

The wave drag coefficient, the deflection angle of the shock wave of the conic part of the body, the dimensionless pressure at the body surface are the same as for the circular cone, whose length is equal to $L_v = L_c + R/\sin\beta_c - R$. The radii h_c and H_{sh} are calculated as $h_c = L_v \operatorname{tg}\beta_c$ and $H_{sh} = L_v \operatorname{tg}\theta_{sh}$, as well as the shock layer thickness $\Delta = H_{sh} - h_c$. The stagnation temperature is found by the known relation [1, 2, 13]:

$$T_{c0} = T_\infty(1 + 0.5(\gamma-1)M^2). \tag{7}$$

The wave drag coefficient of the cone with the spherical nose is determined as $C_{pc} = 0.5C_{p0}(1+\sin^2\beta_c)d^2 + c_{p,c}(1-d^2)$ where $c_{p,c}$ is the wave drag coefficient of the circular cone, whose length is equal to L_v and $d = R\cos\beta_c / h_c$. The pressure coefficient C_{p0} is determined similar to the sphere body at the stagnation point: $C_{p0} = 2 - (\gamma-1)/(\gamma+1) - 2/[(\gamma+1)M^2]$.

For comparison of the results obtained by the analytical formulas and the CFD technique, the supersonic inviscid gas flow around the cone with the spherical blunt nose ($\beta_c = 20^o$, $L_v = 1$ m, $R = 0.048087$ m) was considered ($\gamma = 1.4$, $T_\infty = 216$ K, $P_\infty = 5474$ Pa). Numerical computations showed that the pressure growth in the shock layer (near the vertex of the spherical nose) coincides with the same for a sphere and is determined only by incoming flow Mach number values. The dimensionless pressure P_{c0}/P_∞ falls from 61 (spherical nose) to 9.2 characteristic for conical flows (Fig. 3, *a*).

The calculated stagnation temperature and shock layer thickness for the cone with the spherical nose were compared with the same obtained from formulas (6) and (7) (Tab. 2). As a result, expressions (6) and (7) can be recommended for verification and estimation of numerical mesh features.

Table 2. **Stagnation temperature and the shock layer thickness for the cone with the spherical nose**

M	β_c, ^{o}	T_0, K		Δ_0, m	
		Fluent	Formula (7)	Fluent	Formula (6)
5	20	≈ 1306	1296	≈ 0.007621	0.00751
7	20	≈ 2345	2332.8	≈ 0.00702	0.00693

Truncated cone. A truncated cone is a particular case of bodies with a blunt nose, i. e., those having an aerodynamic shape, around which the flow is accompanied by the formation of a curvilinear shock wave, the development of local sub-and supersonic zones, internal shock waves. The wave drag coefficient of the truncated cone is found as [17]

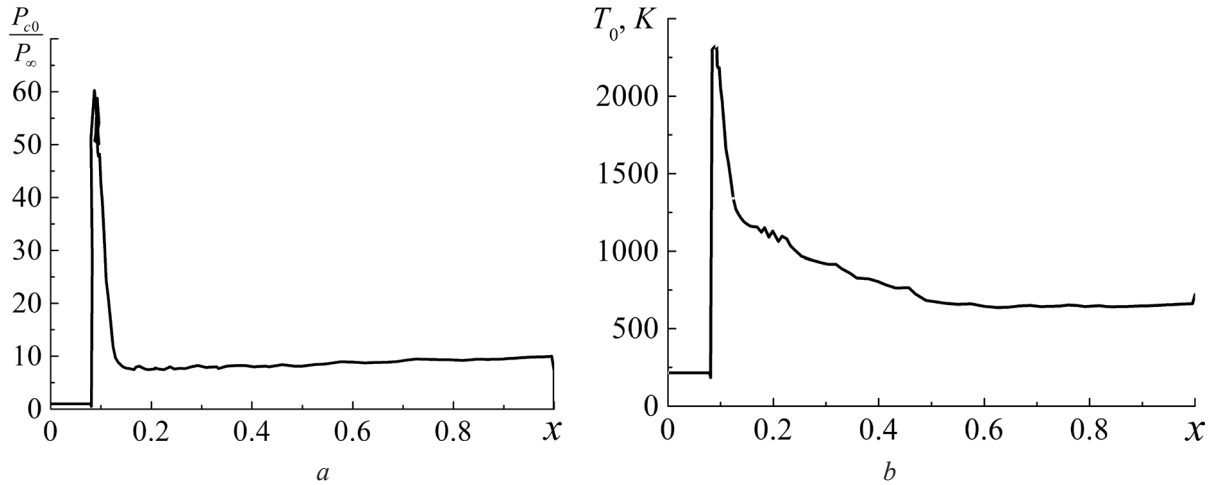

a *b*

Fig. 3. Dimensionless pressure (*a*) and temperature (*b*) in the shock layer around the cone with the spherical nose (CFD data): $\beta_c = 20^o$, $M = 7$

$$C_{pc} = 0.915 C_{p0}(1 + \sin^2 \beta_c) d^2 + c_{p,c}(1 - d^2) \quad (8)$$

where $d = h_0 \cos \beta_c / h_c$.

One of the important flow characteristics is a distance Δ_0, at which the shock wave departs from the head of the truncated cone. For comparison, the following empirical relations are used:

$$\Delta_0 / 2h_0 = 0.23\sqrt{(M^2 + 5)/(M^2 - 1)}, \quad (9)$$

$$\Delta_0 / h_0 = 1.03\sqrt{\rho_\infty / (\rho_{c0} - \rho_\infty)}. \quad (10)$$

The wave drag coefficient, the deflection angle of the shock wave, and the dimensionless pressure of the conical part of the truncated cone are the same as for the circular cone, whose length is equal to L_v.

ANSYS Fluent 14.5 [15] was used to perform numerical computations and to compare them with the experimental data [17]. The diameter of the cone tail is $d_{con} = 2h_c = 30$ mm, the diameter of the cone nose is $h_0 = 2\ h_c/3$, and the half-angle is $\beta_c = 20^o$. The calculated stagnation temperature and shock layer thickness for the truncated cone were compared with the same obtained from formulas (7), (9) and (10). As a result, these parameters found from the numerical analysis are in a good agreement with the analytical values of formulas (7), (9) and (10) (Tab. 3).

Table 3. **Stagnation temperature and the shock layer thickness for the truncated cone**

M	T_0, K Formula (7)	T_0, K, Fluent	Δ_0, m Fluent	Δ_0, m Formula (9)	Δ_0, m Formula (10)
5	1296.0	≈1300.0	≈0.00495	0.00510	≈0.00486
7	2332.8	≈2337.6	≈0.00480	0.00488	≈0.00466

Conclusions. The numerical data for wave drag coefficient, stagnation temperature, and shock layer thickness were used to show a good agreement between the numerical and empirical solutions for supersonic flow around the circular cone, the circular cone with the spherical nose, and the truncated cone. Through this computational analysis, a better interpretation of these physical phenomena can be made. One can conclude that the used empirical solutions can be recommended for CFD software verification and estimation of numerical mesh features. It all is capable of predicting accurate results and also of capturing flow discontinuities, e.g., oblique shock waves and contact surfaces.

References

1. *Chernyi G. G., Losev S. A., Macheret S. O.* et al. Physical and Chemical Processes in Gas Dynamics. Virginia, 2004.
2. *Anderson, J. D., Jr.* Modern Compressible Flow. New York, 2002.
3. *Alhussan K.* Direct fluid–fluid interaction in three-dimensional supersonic non-steady flow. DSc. Diss. The George Washington University, 2002.
4. *Alhussan K.* Computational analysis of high speed flow over a conical surface for air as working fluid // Proc. 3rd IASME/WSEAS Int. Conf. on Fluid Dynamics & Aerodynamics, Corfu, Greece, Aug. 20–22. Corfu, 2005. P. 202–205.
5. *Krasnov N. F.* Aerodynamics of bodies of revolution. Moscow, 1958.
6. *Krasnov N. F.* Fundamentals of estimated aerodynamics. Moscow, 1981.
7. *Hill J. C.* // AIAA J. 1968. Vol. 7, no. 1. P. 165–167.
8. *Simon W. E., Walter L. A.* // AIAA J. 1963. Vol. 1, no. 7. P. 1696–1698.
9. *Nielsen J. N.* Missile aerodynamics. New York, 1988.
10. *Sims J. R.* Tables of supersonic flow around right circular cones at zero angle of attack. NASA-SP-3004. 1964.
11. Equations, Tables, and Charts for Compressible Flow (by Ames Research Staff). NASA Report 1135. 1953.
12. *Bartlett M. A.* Tables of supersonic symmetrical flow around right circular cones, with and without the addition of heat at the wave. R&M. 1968. No. 3521. London: Her Majesty's Stationary Office.
13. *Hase U. D., Probstin R. F.* Theory of supersonic flows. Moscow, 1962.
14. *Barnette D. W.* Program SHOCKS: Quickly estimating super- and hypersonic flows. New Mexico: Sandia National Laboratories, 1993.
15. ANSYS Fluent Tutorial Guide. Ansys Inc., 2011.
16. *Lunev V. V.* Supersonic aerodynamics. Moscow, 1975.
17. *Brodetsky M. D., Shevchenko A. M.* // Appl. Mech.Tech. Phys. 2003. Vol. 44, no. 5. P. 46–55.

Х. АЛЬХУССАН, Т. В. СИДОРОВИЧ, А. Д. ЧОРНЫЙ

СВЕРХЗВУКОВОЙ НЕВЯЗКИЙ ПОТОК ОКОЛО ТЕЛ ВРАЩЕНИЯ: ЭМПИРИЧЕСКИЙ И ЧИСЛЕННЫЙ РАСЧЕТ

Резюме

Расчетные данные по волновому коэффициенту сопротивления, температуре торможения, толщине ударного слоя и другим газодинамическим параметрам были использованы для того, чтобы показать приемлемое согласие между численными и эмпирическими результатами для обтекания сверхзвуковым потоком заостренного кругового конуса, кругового конуса со сферическим носиком и усеченного конуса. Из анализа численных данных, позволяющих получить представление о рассмотренных физических явлениях, можно сделать вывод, что использованные эмпирические соотношения могут быть рекомендованы для верификации разрабатываемого нового программного обеспечения вычислительной гидрогазодинамики, а также для оценки свойств применяемых вычислительных сеток. Это позволяет получать более точные результаты, а также разрешить такие особенности сверхзвукового потока, как ударные волны и контактные границы.